Dramatically Enhanced Fluorescence of Heteroaromatic Chromophores upon Insertion as Spacers into Oligo(triacetylene)s

by **Michael J. Edelmann**, **Jean-Manuel Raimundo**, **Nils F. Utesch**, and **François Diederich***

Laboratorium für Organische Chemie, ETH-Hönggerberg, HCI, CH-8093 Zürich

and

Corinne Boudon, **Jean-Paul Gisselbrecht**, and **Maurice Gross**

Laboratoire d'Electrochimie et de Chimie Physique du Corps Solide, Faculté de Chimie, Université Louis Pasteur and CNRS, UMR no. 7512, 4, rue Blaise Pascal, F-67000 Strasbourg

Dedicated to Professor *David N. Reinhoudt* on the occasion of his 60th birthday

In continuation of a previous study on the modulation of π-electron conjugation of oligo(triacetylene)s by insertion of central hetero-spacer fragments between two (*E*)-hex-3-ene-1,5-diyne ((*E*)-1,2-diethynylethene, DEE) moieties (*Fig. 1*), a new series of trimeric hybrid oligomers (**14**–**18** and **22**–**24**, *Fig. 2*) were prepared (*Schemes 1–3*). Spacers used were both electron-deficient (quinoxaline-based heterocycles, pyridazine) and electron-rich (2,2′-bithiophene, 9,9-dioctyl-9*H*-fluorene) chromophores. With **19**–**21** (*Scheme 4*), a series of transition metal complexes was synthesized as potential precursors for nanoscale scaffolding based on both covalent acetylenic coupling and supramolecular assembly. The UV/VIS spectra (*Fig. 3*) revealed that the majority of spacers provided hetero-trimers featuring extended π-electron delocalization. The new hybrid chromophores show a dramatically enhanced fluorescence compared with the DEE dimer **13** and homo-trimer **12** (*Fig. 5*). This increase in emission intensity appears as a general feature of these systems: even if the spacer molecule is non-fluorescent, the corresponding hetero-trimer may show a strong emission (*Table 2*). The redox properties of the new hybrid chromophores were determined by cyclic voltammetry (CV) and rotating-disk voltammetry (RDV) (*Table 3* and *Fig. 5*). In each case, the first one-electron reduction step in the hetero-trimers appeared anodically shifted compared with DEE dimer **13** and homo-trimer **12**. With larger spacer chromophore extending into two dimensions (as in **14**–**18**, *Fig. 2*), the anodic shift (by 240–490 mV, *Table 3*) seems to originate from inductive effects of the two strongly electron-accepting DEE substituents rather than from extended π-electron conjugation along the oligomeric backbone, as had previously been observed for DEE-substituted porphyrins.

Introduction. – In a previous study, we had explored how the properties of oligomers made from (*E*)-1,2-diethynylethene (DEE, (*E*)-hex-3-ene-1,5-diyne) repeating units can be tuned or changed by the insertion of spacer chromophores [1]. For this purpose, a series of eleven hybrid oligomers **1**–**11** (*Fig. 1*) were prepared, in which mostly aromatic hetero-spacers with different electronic characteristics were introduced between two DEE moieties. UV/VIS Studies revealed that the majority of the hetero-spacers were less effective than the homo-spacer DEE in trimeric **12** in facilitating π-electron delocalization along the linear conjugated oligomeric backbone. Electrochemical investigations by cyclic voltammetry (CV) and rotating-disk voltammetry (RDV) confirmed these results.

On the other hand, fluorescence studies clearly demonstrated that a desirable function can be created or strongly enhanced upon insertion of hetero-spacers into pure DEE oligomers [2–4]. Thus, the heterocyclic derivatives **7**–**9**, containing pyridine, pyrazine, or thiophene spacers, respectively, feature a strong fluorescence emission, which is present to a significant extent neither in the DEE homo-trimer **12** or dimer **13** nor in the individual hetero-aromatic spacer component.

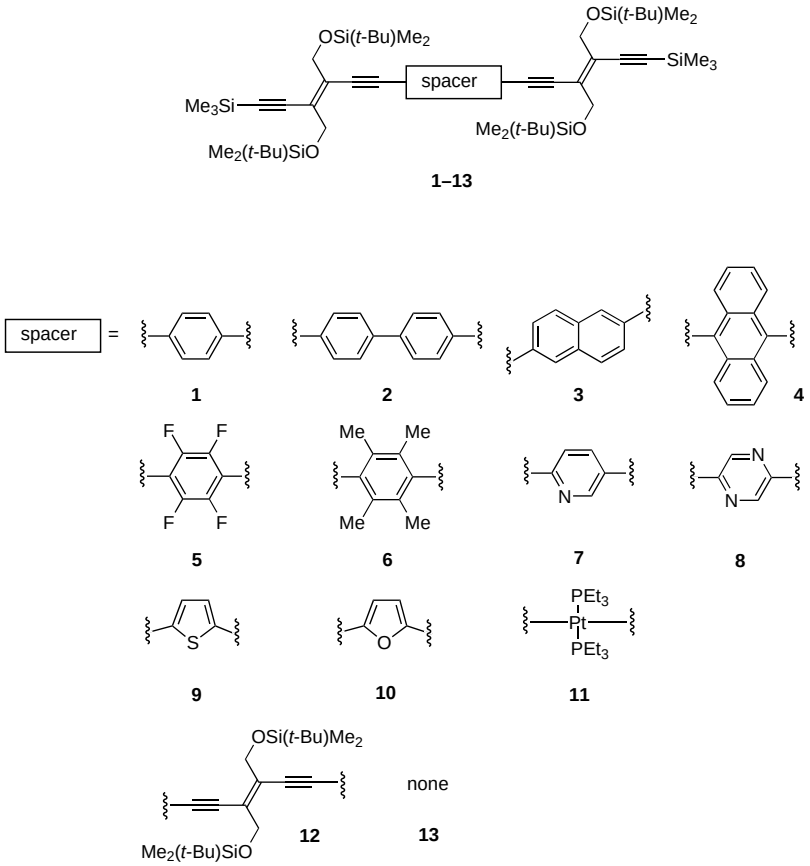

Fig. 1. *First series of trimeric hybrid oligomers prepared by incorporation of different hetero-spacers between two DEE moieties* [1]

The hybrid oligomers were subsequently found to be valid models for extrapolating the properties of the corresponding longer-chain polymers [5]. *Hay* oligomerization [6] of terminally bis-deprotected **2** provided two soluble polymers (degrees of polymerization $X_n = 19$ (16900 Dalton) and 23 (20600 Dalton)), which exhibited fluorescence emissions (fluorescence quantum yields $\Phi_F = 0.44$ and 0.51, resp.) of nearly similar intensity to that measured for the hybrid trimer ($\Phi_F = 0.73$).

Encouraged by these results, we engaged in the preparation of a novel series of hybrid trimers and related transition metal complexes featuring both electron-deficient spacers (such as quinoxaline-based heterocycles (in **14**–**21**) or pyridazine (**22**)) and electron-rich spacers (such as 2,2′-bithiophene (**23**) and 9,9-dioctyl-9*H*-fluorene (**24**); *Fig. 2*). We show, by UV/VIS and electrochemical studies, that the electronic properties of the hetero-trimers strongly depend on the nature of the spacer chromophore. Furthermore, we provide evidence that a dramatically enhanced fluorescence intensity (compared with DEE dimer **13**, homo-trimer **12** or the parent spacer) is a general characteristic of this type of hetero-trimeric oligomers.

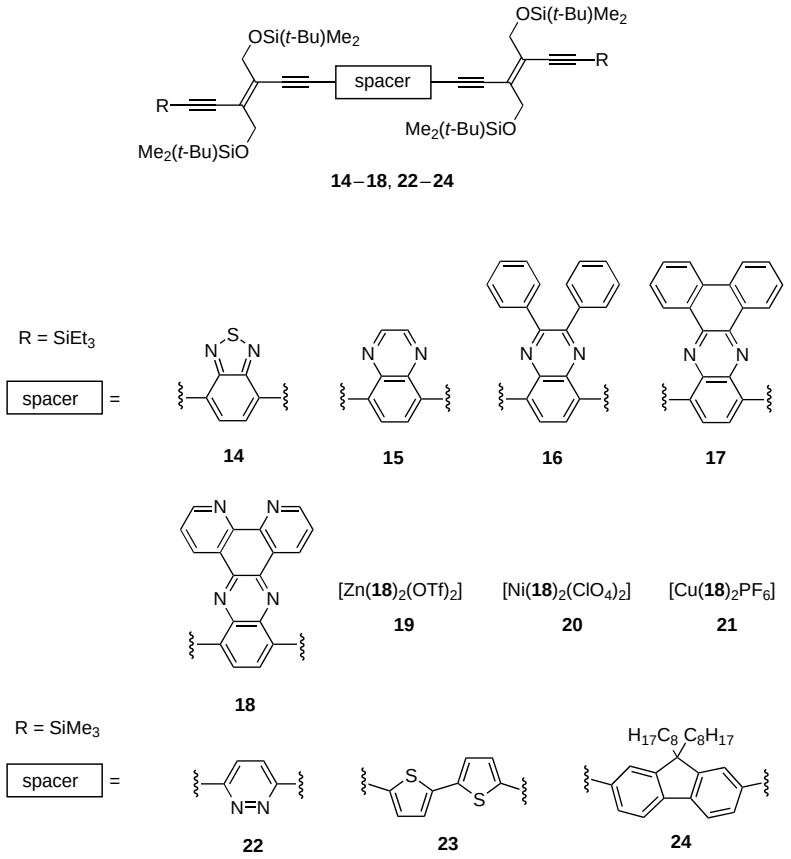

Fig. 2. *New series of trimeric hybrid oligomers obtained by insertion of spacer chromophores into two DEE units*

Results and Discussion. – 2.1. *Synthesis.* The key step in the synthesis of the new hetero-trimers **14**–**18** and **22**–**24** was the Pd-catalyzed *Sonogashira* cross-coupling reaction [7] with 2 equiv. of monoprotected DEE **25** (R = Et_3Si) or **26** (R = Me_3Si), and the appropriately dihalogenated spacer derivative **27**–**34** (*Scheme 1*). The detailed reaction conditions are listed in *Table 1*. As a side product, these reactions afforded small quantities of Me_3Si- (**13**) or Et_3Si-end-capped DEE dimer (usually *ca.* 5%) because of homo-coupling of **26** and **25**, respectively. Yields in the double cross-coupling reaction varied between 27 and 85%, with electron-deficient dihalides being the best coupling partners, a previously shown trend [8]. An unexpectedly low yield of 27% was obtained in the coupling of 3,6-diiodopyridazine due to problems with the purification of **22**.

The synthesis of the dihalogenated spacer precursors **27**–**34** is summarized in *Schemes 2* and *3*. Compound **27** was prepared in high yield (88%) by bromination of commercially available 2,1,3-benzothiadiazole (**35**). Reduction of **27** with $NaBH_4$ gave 1,2-diamine **36** that was condensed with appropriate 1,2-dicarbonyl derivatives to give

Scheme 1. *General Preparation of the Hybrid Oligomers* **14**–**18** *and* **22**–**24**. The detailed reaction conditions are listed in *Table 1*.

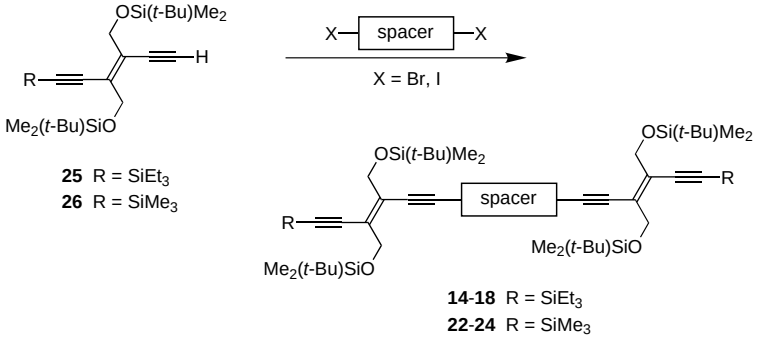

Table 1. *Reaction Conditions for the Cross-Coupling of DEEs* **25** *or* **26** *with the Bis-Functionalized Chromophores X-Spacer-X Affording the Hybrid Oligomers* **14**–**18** *and* **22**–**24**

Compound	DEE	X-Spacer-X [a])	Reaction conditions	Yield [%]
14	**25** [b])	**27**	CH_2Cl_2/NEt_3 1:1, r.t., 18 h [c])	70
15	**25** [b])	**28**	CH_2Cl_2/NEt_3 1:1, r.t., 18 h [c])	48
16	**25** [b])	**29**	CH_2Cl_2/NEt_3 1:1, reflux, 18 h [c])	43
17	**25** [b])	**30**	CH_2Cl_2/NEt_3 1:1, reflux, 18 h [c])	56
18	**25** [d])	**31**	CH_2Cl_2/NEt_3 2:1, reflux, 18 h [e])	65
22	**26** [d])	**33**	THF/$(i\text{-}Pr)_2NH$, 60°, 21 h [c])	27
23	**26** [d])	**32**	PhMe/NEt_3, 60°, 48 h [e])	52
24	**26** [b])	**34**	NEt_3, 70°, 23 h [f])	85

[a]) 1 Equiv. was used. [b]) 2.4 Equiv. were used. [c]) $[PdCl_2(PPh_3)_2]$ (5 mol-%) and CuI (6 mol-%) were employed as catalysts under an Ar atmosphere. [d]) 2.0 Equiv. were used. [e]) $[PdCl_2(PPh_3)_2]$ (3 mol-%) and CuI (7 mol-%) under Ar. [f]) $[PdCl_2(PPh_3)_2]$ (1.2 mol-%) and CuI (2.4 mol-%) under Ar.

the quinoxaline-based spacers (glyoxal → **28**; benzyl → **29**; phenanthrene-9,10-dione → **30**; 1,10-phenanthroline-5,6-dione (**37**) → **31**) [9–11]. Compound **37** was synthesized in 22% yield by oxidizing 1,10-phenanthroline (**38**) with bleach and then heating to reflux in a mixture of aqueous H_2SO_4/HNO_3 [10][12–15].

The 2,2′-bithiophene spacer **32** was prepared by iodination of commercially available 2,2′-bithiophene (**39**; *Scheme 3*) [16]. The pyridazine spacer **33** was synthesized *via* a route starting from maleic anhydride (**40**) [17][18]; treatment with $N_2H_4 \cdot HCl$ yielded hydrazide **41** that was transformed into **33** by two consecutive aromatic nucleophilic substitutions with $POCl_3$ and ICl/HI. Compound **34** was obtained by dialkylation of 2,7-dibromo-9*H*-fluorene (**42**) [19][20].

The new hybrid oligomers **14**–**18** and **22**–**24** were isolated as solids that melt without decomposition and are stable to light exposure and air under standard laboratory conditions.

Complexation of the bidentate 1,10-phenanthroline-type ligand in **18** with transition-metal ions (Zn^{2+}, Ni^{2+}, and Cu^{+}) provided complexes **19**–**21**, potential building blocks for ladder-type oligomers or polymers. Formation of **19**–**21** was

Scheme 2. *Synthesis of the Halogenated Spacer Compou*nds **27**–**31**

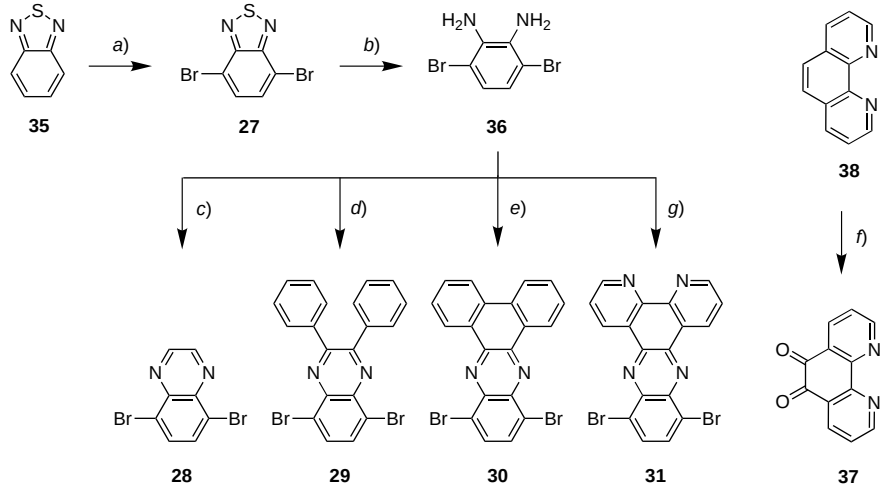

a) Br_2, HBr (48% in H_2O), Δ, 2 h; 88%. *b*) $NaBH_4$, EtOH, 0° → r.t., 20 h; 87%. *c*) Glyoxal (40% in H_2O), EtOH, Δ, 3 h; 40%. *d*) Benzil, EtOH, Δ, 1 h; 70%. *e*) Phenanthrene-9,10-dione, EtOH/AcOH 20:1, Δ, 2 h; 80%. *f*) i) 1,10-Phenanthroline, bleach, $CHCl_3$, 6 h; ii) $H_2SO_4/HNO_3/H_2O$, Δ, 6 h; 22%. *g*) **37**, EtOH, Δ, 3 h; 91%.

Scheme 3. *Synthesis of the Halogenated Spacer Compounds* **32**–**34**

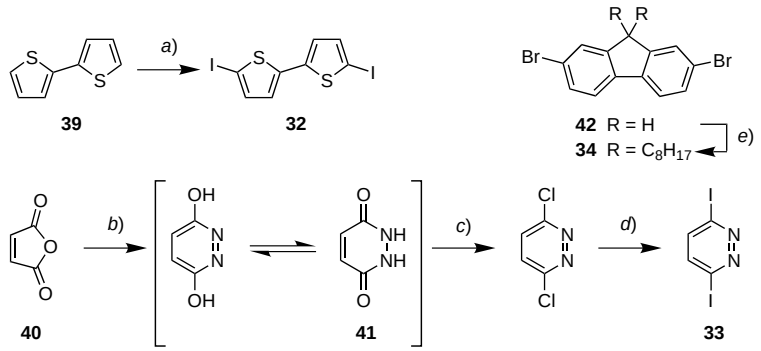

a) HgO, I_2, PhH, 0° → r.t., 24 h; 48%. *b*) $N_2H_4 \cdot 2$ HCl, H_2O, 100°, 3 h; 92%. *c*) $POCl_3$, Δ, 5 h; 67%. *d*) ICl, HI (55% in H_2O), 70°, 24 h; 50%. *e*) NaOH (50% in H_2O), $C_8H_{17}Br$, $PhCH_2NEt_3Cl$, Me_2SO, r.t., 2 h; 65%.

accomplished by stirring **18** (2 equiv.) with $Zn(OTf)_2$ (OTf = OSO_2CF_3), $Ni(ClO_4)_2$, or $[CuPF_6(MeCN)_4]$ (1 equiv.) in $MeOH/CH_2Cl_2$ in the dark under Ar at room temperature (*Scheme 4*). Evaporation *in vacuo* and precipitation from MeOH yielded the desired complexes **19**, **20**, and **21** in 64, 71, and 58% yield, respectively, as stable red solids, which were readily soluble in organic solvents such as $CHCl_3$, CH_2Cl_2, or THF and decompose only upon heating above 250°.

The complexes were characterized by mass spectrometry, UV/VIS and IR spectroscopy and, in the case of the Zn^{2+} complex **19**, also by NMR spectroscopy.

Scheme 4. *Synthesis of the Transition Metal Complexes* **19**–**21**

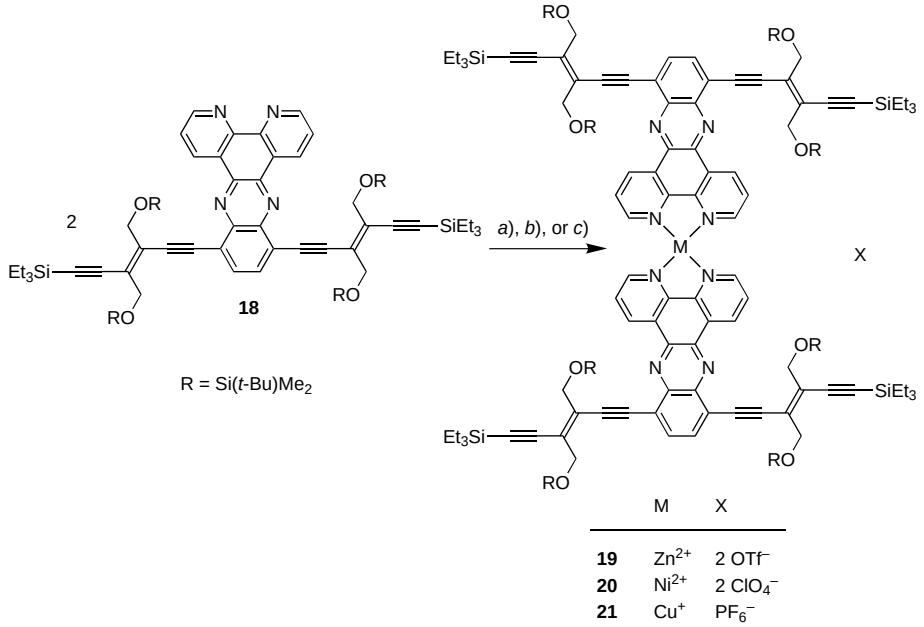

a) $Zn(OTf)_2$, $MeOH/CH_2Cl_2$, r.t., 16 h; 64%. *b)* $[Ni(ClO_4)_2 \cdot 6\ H_2O]$, $MeOH/CH_2Cl_2$, r.t., 16 h; 71%. *c)* $[CuPF_6(MeCN)_4]$, $MeOH/CH_2Cl_2$, r.t., 16 h; 58%.

The matrix-assisted laser-desorption-ionization time-of-flight mass spectrum (MALDI-TOF-MS; matrix: 2,5-dihydroxybenzoic acid (DHB)) of **19** showed the $[M + H - OTf]^+$ ion as parent ion. Similarly, the spectrum of **20** displayed the $[M - 2\ ClO_4 + Cl]^+$ ion as the major peak besides strong signals for $[M - ClO_4]^+$ (36%) and $[M - 2\ ClO_4]^+$ (74%), whereas the spectrum of **21** featured the $[M - PF_6]^+$ ion as the most prominent ion.

The Ni^{2+} complex **20** gave broad signals in the ^{1}H-NMR spectrum, pointing to a paramagnetic species. Ni^{2+} (d^8-electron configuration) can exist either in a diamagnetic square-planar low-spin or in a paramagnetic tetrahedral high-spin form [21]. Complex **20**, therefore, seems to exist in the latter form. Although complex **21** includes a Cu^+ center with d^{10}-electron configuration, its characterization by NMR spectroscopy was inhibited by traces of paramagnetic Cu^{2+} species. Only the diamagnetic Zn^{2+} complex **19** (d^{10}-electron configuration) was fully characterized by ^{1}H- and ^{13}C-NMR spectroscopy. For **19** and **21**, we also postulate a tetrahedral coordination geometry, which should be favored over a square-planar array for steric reasons. In a tetrahedral complex, the two hetero-trimer rods stay perpendicular to each other, gaining more space for the bulky (*t*-Bu)Me_2SiO side chains.

2.2. *UV/VIS Studies.* The electronic absorption spectra of the new hybrid compounds **14**–**17** in CH_2Cl_2 and **18**–**24** in $CHCl_3$ are shown in *Fig. 3* together with those of the DEE dimer **13** and homo-trimer **12**. In contrast to the previously

investigated series of hetero-trimers **1**–**11** (with the exception of anthracene derivative **4**; *Fig. 1*), the position of the longest wavelength absorption maxima λ_{max} (*Table 2*) does not correlate in a straightforward way with the extent of π-electron delocalization along the oligomeric hetero-trimeric backbone.

Table 2. *UV/VIS and Fluorescence Data of Hetero-Trimers* **14**–**18** *and* **22**–**24**, *Transition Metal Complexes* **19**–**21** *and, for Comparison, the Pure DEE Oligomers* **12** *and* **13**. Spectra recorded at room temperature in $CHCl_3$, except indicated otherwise.

Compound	λ_{max} [nm] [a] (ε [M^{-1} cm^{-1}] [b])	End absorption [nm] [c]	λ_{exc} [nm] [d] (ε [M^{-1} cm^{-1}] [b])	λ_{em} [nm] [e]	Φ_F [f]
12	407 (sh, 36700)	460	356 (31800)	399, 440	0.01
13	376 (24700)	415	356 (25300)	425	0.01
14 [g]	438 (35900)	525	400 (20500)	522	0.80
15 [g]	436 (sh, 22300)	480	400 (30200)	490	0.65
16 [g]	435 (sh, 24100)	500	400 (28900)	487	0.72
17 [g]	445 (21300)	525	400 (20100)	526	0.75
18	462 (25800)	550	354 (56800)	543	0.68
19	471 (28900)	600	354 (89300)	552	0.17
20	485 (32400)	600	354 (127600)	578	0.03
21	469 (42500)	600	354 (126800)	545	0.33
22	372 (sh, 31900)	420	– [h]	– [h]	– [h]
23	442 (sh, 15700)	490	350 (12700)	472	0.13
24	393 (sh, 46500)	440	350 (39900)	409	0.39
43	312 (13300)	375	312 (13300)	345, 373	0.027
44 [i]	315 (6500)	350	313	398	0.0002
45 [i]	348 (11700)	400	313	410	0.0059
46	400 (41700) [j]	$\approx$ 450 [j]	365 [k]	–	0.12 [k]
47	380 (12700)	420	354 (8500)	– [h]	– [h]

[a]) Experimentally observed longest-wavelength absorption maxima. [b]) Molar extinction coefficient. [c]) Experimentally observed wavelength at which the absorption reaches $\varepsilon = 0$ M^{-1} cm^{-1}. [d]) Excitation wavelength. [e]) Fluorescence emission band. [f]) Fluorescence quantum yield: Anthracene ($\Phi_F = 0.33$ in hexane) was used as reference compound [25]. [g]) In CH_2Cl_2. [h]) Not fluorescent. [i]) In EtOH, taken from [23]. [j]) In EtOH, 90 K, taken from [24]. [k]) In PhH, taken from [22].

On one hand, the spectra of **22**–**24** resemble in their shape those of DEE derivatives **12** and **13**, indicating that π-electron delocalization along the oligomeric backbone determines the position of λ_{max}. The particular efficiency of the 2,2′-bithiophene moiety in facilitating this conjugation pathway is noticeable. The longest-wavelength absorption maximum of hetero-trimer **23** (442 nm) features a substantial bathochromic shift when compared to DEE homo-trimer **12** (407 nm), presumably as a result of intramolecular donor-acceptor interactions between the electron-rich spacer and the electron-deficient DEE moieties [1]. The pyridazine and 9,9-dioctyl-9*H*-fluorene spacers are much less efficient in facilitating π-electron delocalization.

On the other hand, the spectra of **14**–**18** (and the corresponding metal complexes **19**–**21**) are very different and no longer resemble those of DEE derivatives **12** and **13**. They feature broad longest-wavelength absorption bands that are substantially red-shifted as compared with the spectra of **12**, **13**, and also **22**–**24**. The central spacer components in these hetero-trimers extend substantially into two dimensions, and the

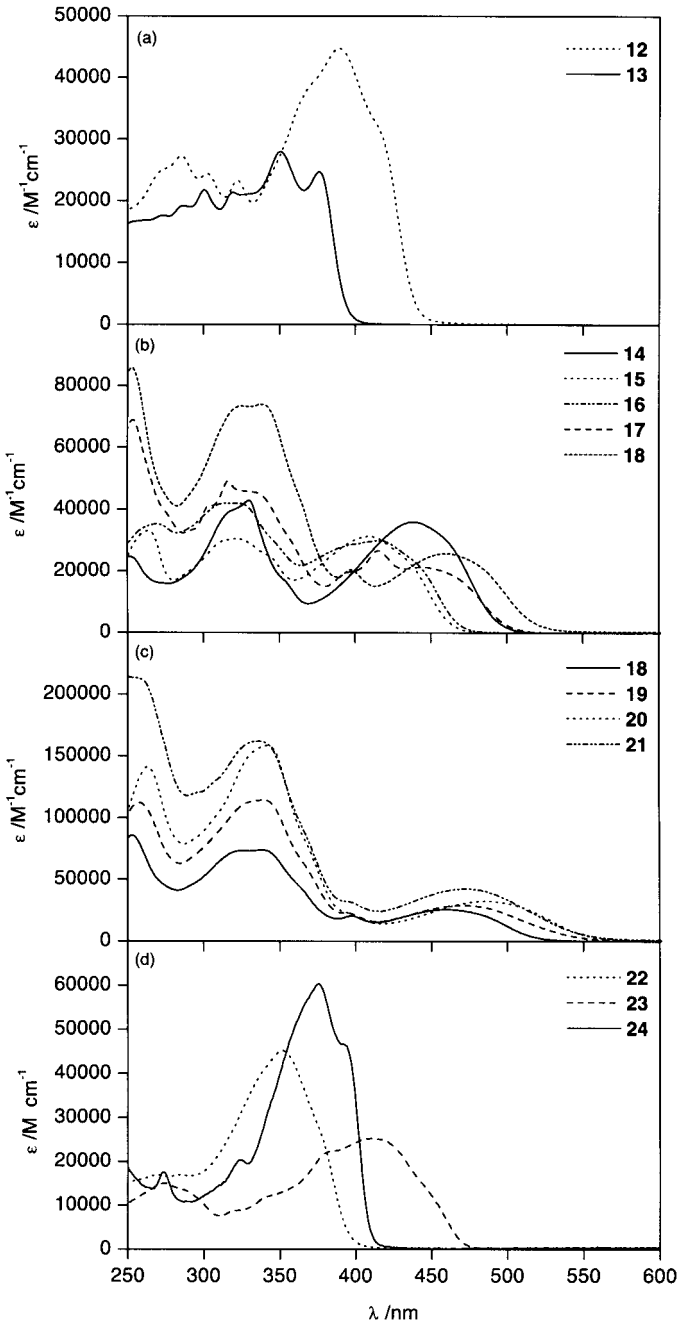

Fig. 3. *UV/VIS Spectra of* a) *DEE dimer* **13** *and homo-trimer* **12** *in* $CHCl_3$, b) *hetero-trimers* **14**–**17** *in* CH_2Cl_2 *and* **18** *in* $CHCl_3$, c) *transition metal complexes* **19**–**21** *in* $CHCl_3$, *and* d) *hetero-trimers* **22**–**24** *in* $CHCl_3$

longest-wavelength bands presumably result from electronic transitions mainly involving the π-system within the spacer chromophore. A similar spectral behavior had already been observed for anthracene derivative **4**, which featured bathochromically shifted, typical 'anthracene'-type absorption bands rather than bands resembling those of DEE oligomers [1].

A comparison of the spectra of the pure spacer chromophores **43**–**47** (*Fig. 4*) with those of the corresponding hetero-trimers **15**–**18**, respectively, shows that a substantial bathochromic shift of the longest-wavelength absorption maximum results from attachment of the two DEE moieties to the central spacer and the concomitant extension of π-electron delocalization. The difference in energy between the bands of the free and bis-DEE-substituted spacer decreases with increasing spacer size. Thus, the longest-wavelength absorption maxima λ_{max} shift bathochromically from 315 nm (**44** in EtOH) [23] to 436 nm (**15**, difference in energy between the two transitions: $\Delta E = 1.09$ eV), from 348 nm (**45** in EtOH) [23] to 435 nm (**16**, $\Delta E = 0.71$ eV), from 400 nm (**46** in EtOH) [24] to 445 nm (**17**, $\Delta E = 0.32$ eV), and from 380 nm (**47** in $CHCl_3$) to 462 nm (**18**, $\Delta E = 0.58$ eV). This comparison does not take into account solvatochromic shifts, which should be negligible in the systems considered. Metal-ion complexation induces a further red-shift of the longest-wavelength absorption maximum ($\lambda_{max} = 471$ (**19**), 485 (**20**), and 469 (**21**) nm) compared to the free hetero-trimer **18** (462 nm). Future theoretical calculations would be worthwhile to shed further light on the nature and polarization of the longest-wavelength transitions in the various types of hetero-trimers.

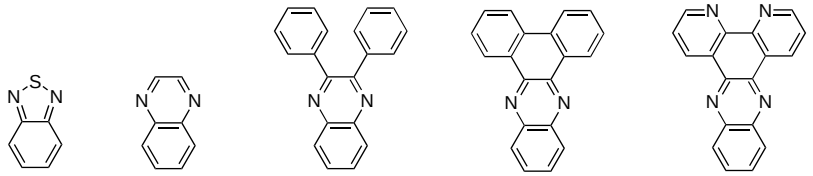

Fig. 4. *Spacer chromophores* **43**–**47** *for spectral comparison with hetero-trimers* **14**–**18**

2.3. *Fluorescence Studies.* Fluorescence spectra for **14**–**17** were recorded in CH_2Cl_2 and for **18**–**24** in $CHCl_3$ at room temperature. The fluorescence quantum yields Φ_F were measured relative to anthracene in hexane ($\Phi_F = 0.33$ [25]; *Table 2*). Whereas the DEE dimer **13** and homo-trimer **12** only fluoresce very weakly ($\Phi_F = 0.01$), the majority of the hetero-trimers show a very strong emission with a high fluorescence quantum yield. This is a remarkable property of this unique class of hybrid chromophores, which undoubtedly results from the incorporation of the hetero-spacer into the oligomeric backbone.

The benzothiadiazole-containing oligomer **14** shows by far the highest fluorescence quantum yield ($\Phi_F = 0.80$); its fluorescence spectrum is displayed in *Fig. 5*. A strong emission ($\Phi_F =$ between 0.65 and 0.75) is also observed for the quinoxaline derivatives **15**–**18**. Furthermore, hybrid oligomers **14**–**18** display a strong fluorescence in the solid state and for spin-coated films of **14**, a Φ_F of *ca.* 0.50 was measured.

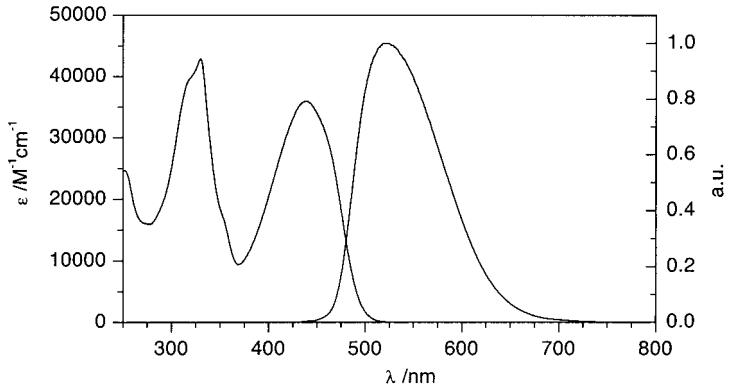

Fig. 5. *Electronic absorption and emission spectra of hetero-trimer* **14** *in* CH_2Cl_2 ($\lambda_{exc} = 400$ nm, $\Phi_F = 0.8$)

Comparative studies demonstrate a dramatic enhancement of the fluorescence intensity upon insertion of a spacer compound into the hetero-trimeric oligomer. The parent spacers **43**–**47** (*Fig. 4*) are only weakly fluorescent or do not emit at all (*Table 2*). Thus, compound **47** does not show any fluorescence in $CHCl_3$, whereas the corresponding hetero-trimer **18** displays a strong emission ($\lambda_{em} = 543$ nm; $\Phi_F = 0.68$). These results complement our earlier findings [1], showing that the introduction of weakly fluorescent heterocycles such as pyridine, pyrazine, or thiophene as spacers into the hetero-trimers **7**–**9**, respectively, gave highly emitting oligomers. We, therefore, conclude that substituting a conjugated π-chromophore with two DEE moieties – under formation of a hetero-trimeric oligomer – is a powerful way to generate strong fluorescence emission.

A change in the overall π-electron conjugation is well-known to influence electronic emission properties [26]. Remarkably, the increase in fluorescence quantum yield occurs despite the presence of the flexible (*t*-Bu)Me_2SiOCH_2 side chains on the DEE moieties. It is empirically well-established that enhanced rigidity of a molecule leads to enhanced luminescence due to a reduced vibrational deactivation of the excited state [27]. Apparently, this does not hold for the hetero-trimers described here. Rather, we propose that the bulky side chains have a favorable steric effect by preventing chromophore aggregation, which is known to reduce the fluorescence efficiency in conjugated oligomers and polymers [28].

Complexation of **18** with transition metal ions under formation of **19**–**21** leads to a red-shift of the emission band and a decrease in the fluorescence quantum yield, which is particularly pronounced in the Ni^{2+} complex **20** ($\Phi_F = 0.03$). Whereas metal-ion coordination may, in some cases, enhance fluorescence emission by rigidification of π-scaffolds, the 'heavy-atom effect' acts counterproductively, by facilitating deactivation of the singlet excited state through intersystem crossing to the triplet state [27].

2.4. *Electrochemical Investigations.* The redox characteristics were investigated by cyclic (CV) and rotating-disk voltammetry (RDV) in CH_2Cl_2 (+0.1M Bu_4NPF_6) with a classical three-electrode cell. The working electrode was a glassy-C electrode (3 mm in diameter), the counter electrode a Pt wire, and the pseudo-reference electrode a Pt

Table 3. *Redox Characteristics of Hybrid Oligomers* **14**–**18** and **22**–**24** *and Complexes* **19**–**21** *in Comparison to DEE Derivatives* **12**,**13** *and Spacers* **43**–**45** *and* **47**, *Determined by Cyclic (CV) and Rotating Disk Voltammetry (RDV) in* CH_2Cl_2.

Compound	CV [a])			RDV [b])	
	E'_o [V] [c]) (ΔE_p [mV]) [d])	E_{pc} [V] [e])	E_{pa} [V] [f])	$E^{red}_{1/2}$ [V] (slope [mV]) [g])	$E^{ox}_{1/2}$ [V] (slope [mV]) [g])
12 [h])	−1.88 (80)	−2.09	+1.29	–	–
13 [h])	−2.10 (130)	–	+1.29	−2.12 (70)	–
14	−1.47 (90)	−2.15 [i])	+1.18	−1.59 (100)	+1.19 (70)
		−2.33		−2.10 (100)	
15	−1.75 (100)	−2.12	+1.17	−1.76 (75)	+1.13 (70)
				−2.17 (75)	
16	−1.72 (100)	−2.08	+1.16	−1.73 (80)	+1.15 (75)
17	−1.54 (90)	–	+1.15	−1.54 (75)	+1.13 (75)
	−1.98 (80)			−1.99 (80)	
18	−1.46 (90)	–	+1.16	−1.47 (80)	+1.15 (75)
	−1.92 (90)			−1.94 (75)	
19	−1.44 (60)	−1.19 [j])	+1.15	−1.20 (125) [j])	−(−)
	−1.90 (75)			−1.95 (75)	
20	−1.47 (−)	−1.26 [j])	+1.23	−1.26 (100) [j])	−(−)
	−1.88 (−)				
21	−1.44 (110)	−1.24 [j])	–	−1.29 (100) [j])	−(−)
	−1.86 (150)			−1.92 (60)	
22	−1.86 (70)	−2.15	–	not resolved	–
23	+0.80 (75)	−2.12	+1.09	+0.78 (75)	–
				+1.10 (110)	
24	+1.05 (100)	−2.35	–	not resolved	+1.07 (65)
43	−1.96 (80)	–	–	–	–
44	−2.15 [i])	–	–	–	–
45	−2.09 (75)	–	–	–	–
47	−1.70 (70)	−2.13	–	–	–

[a]) Potentials *vs.* ferricinium/ferrocene (Fc^+/Fc); glassy C-electrode in CH_2Cl_2 + 0.1M Bu_4NPF_6, scan rate ν = 0.1 V s^{-1}. [b]) Potentials *vs.* Fc^+/Fc, rotating-disk electrode in CH_2Cl_2 + 0.1M Bu_4NPF_6. [c]) Formal redox potential $E'_o = (E_{pa} + E_{pc})/2$. The subscripts pa and pc refer to the conjugated oxidation and reduction peaks, respectively. [d]) Peak splitting $\Delta E_p = E_{pa} - E_{pc}$. [e]) Peak potential E_{pc} for irreversible reduction. [f]) Peak potential E_{pa} for irreversible oxidation. [g]) Logarithmic analysis of the wave obtained by plotting E *vs.* $\log[I/(I_{lim} - I)]$. [h]) Taken from [1]. i) Reversible electron transfer at scan rates $\nu > 1$ V s^{-1}. [j]) Adsorption peak (CV) or wave (RDV).

wire. All potentials are referred to ferrocene used as an internal standard, and the results are summarized in *Table 3*.

The derivatives with a quinoxaline spacer **14**–**18** all gave an irreversible oxidation step at about constant potential ($E_{pa} = +1.16$ V), quite similar to the previously studied oligomers **3**, **6**, **12**, and **13** ([1], E_{pa} between +1.29 and +1.17 V). On the other hand, the first reduction of the hetero-oligomers **14**–**18** is substantially facilitated (by 130–420 mV) with respect to the DEE homo-trimer **12**.

A comparison of the reduction potentials of the hetero-oligomers with those of the pure spacer compounds provided interesting information. Hetero-trimer **14** is reversibly reduced in a one-electron step at −1.47 V, which corresponds to an anodic shift of 490 mV compared to the reduction potential of the free benzothiadiazole spacer **43**. The first reduction step in the quinoxaline-derived series, involving one

electron, behaves as quasi-reversible electron transfer with a potential shift to less-negative values, following the sequence **15** → **16** → **17** → **18** (E'_o ranging from −1.75 down to −1.46 V). Again, substantial anodic shifts are observed when comparing to the first reduction potentials of the free spacers, with potential differences of 400 mV (**44** → **15**), 370 mV (**45** → **16**), and 240 mV (**47** → **18**). These large potential shifts are reminiscent of the previously observed anodic shift of the first reduction potential (350 mV) of a porphyrin derivative upon substitution by two DEE moieties in opposite *meso*-positions [29]. We propose that the large anodic-potential shifts measured for these hetero-trimers originate predominantly from inductive effects of the two strongly electron-accepting DEE substituents on the large central-spacer chromophore rather than from extended π-electron conjugation along the oligomeric backbone. This hypothesis is also supported by the UV/VIS spectra of **14**–**18**, which do not feature shapes and bands characteristic for DEE oligomers (*Fig. 3*).

In contrast, the insertion of smaller spacers that extend mainly along the oligomeric backbone does not induce anodic shifts of the first reduction potential when compared to DEE homo-trimer **12**. This behavior of small spacers had already been observed in our previous study [1]. Thus, the pyridazine oligomer **22** is reduced at a potential (−1.86 V) similar to that measured for homo-trimer **12** (−1.88 V). 2,2′-Bithiophene-containing trimer **23** is even more difficult to reduce than DEE homo-trimer **12**, and its first reduction ($E_{pc} = -2.12$ V) occurs close to that of the DEE dimer **13** ($E'_o = -2.10$ V). For **24**, the reduction is even less favorable ($E_{pc} = -2.35$ V), confirming the UV/VIS data that π-electron conjugation through the fluorene spacer is not very efficient. Compounds **23** and **24** also feature each a spacer-centered reversible one-electron oxidation step. In the 2,2′-bithiophene-containing oligomer **23**, this oxidation occurs at +0.80 V [30], whereas it appears at +1.24 V in the 9,9-dioctyl-9*H*-fluorene derivative **24**.

The three metal complexes **19**–**21** gave nearly the same electrochemical behavior. As shown for the CV of the Zn^{2+} complex (*Fig. 6*), an irreversible reduction peak was observed before the two reversible steps. CVs at different sweep rates clearly showed that, for the first reduction, the peak current amplitude was increasing with the sweep

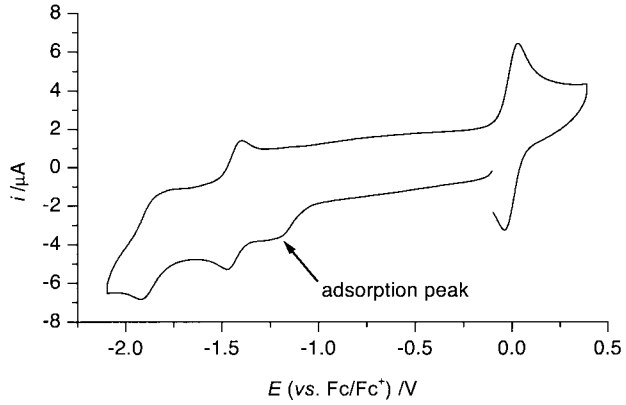

Fig. 6. *Cyclic voltammogram of Zn complex* **19** *in* CH_2Cl_2 *at room temperature in the presence of ferrocene.* Clearly visible is the adsorption peak. All metal complexes studied gave essentially identical electrochemical behavior.

rate, whereas the remaining peak currents were increasing with the square root of the sweep rate. Such behavior in CV clearly indicates that the first reduction step behaves as an adsorption peak. To verify this hypothesis, CVs were run at different temperatures. At lower temperature ($-10°$), the peak current increased, whereas at higher temperature ($30°$), the peak current became much smaller. As the peak current evolution is dependent on $1/T$, it is characteristic of adsorption [31]. Even in rotating-disk voltammetry (RDV), the first reduction, spread out on the potential axis and occurring at -1.20 V, corresponds also to the reduction of strongly adsorbed products. By increasing the temperature up to $30°$, its amplitude decreases, whereas the reduction wave at -1.44 V can be observed. The two reversible electron transfers observed at -1.44 and -1.90 V are similar to those of ligand **18**. The peak characteristics (peak potential difference close to 60 mV) is a good indication that the two ligands in the complex are reduced at the same potentials and behave as independent redox centers.

Conclusions. – This investigation, together with that previously reported [1], has revealed several trends that become apparent when spacer chromophores are inserted between two DEE moieties under formation of hetero-trimeric oligomers. The major result of this study clearly is the demonstration that the fluorescence properties of spacer chromophores – nearly independent on their size and shape – are strongly enhanced in the hybrid oligomers. Fluorescence quantum yields in some cases are dramatically increased by several magnitudes. Thus, compound **47** does not show any fluorescence in $CHCl_3$, whereas the corresponding hetero-trimer **18** displays a strong emission ($\lambda_{em} = 543$ nm; $\Phi_F = 0.68$). The fluorescence quantum yields are not only greatly increased in comparison with the free spacer chromophores but also in comparison with the DEE dimer **13** and homo-trimer **12**, which both show a weak fluorescence ($\Phi_F = 0.01$). We believe that DEE substituents could become useful building modules in electroluminescent materials, enhancing both the solubility and the emission properties of appended chromophores [32]. Also, we expect interesting results from two-photon-absorption studies on oligomers such as those described in this paper [33][34].

The electronic absorption properties and the electrochemical behavior of the hybrid oligomers are strongly dependent on the nature of the central spacer. If the spacer extends in size mainly in the direction of the oligomeric backbone (as in **1**–**3** and **5**–**10**, *Fig 1*; and **22**–**24**, *Fig. 2*), the properties of the resulting oligomers seem to be determined by the extent of π-electron conjugation along this backbone. In this case, the UV/VIS spectra resemble those of the DEE dimer **13** and homo-trimer **12**. Spacers with high benzenoid character such as 9,9-dioctyl-9*H*-fluorene (in **24**) or benzene derivatives (in **1**–**3**, **5**, **6**) are the least efficient in promoting π-electron delocalization along the backbone. The longest-wavelength absorption maxima of the corresponding hetero-trimers are hypsochromically shifted compared to those of DEE trimer **12**, and their first one-electron reduction occurs at more negative potentials than the first reduction of DEE dimer **13**. If, however, the spacer is a larger chromophore, extending into two dimensions (as in **4**, *Fig. 1*, or **14**–**18**, *Fig. 2*), the optical and electrochemical properties seem no longer to be controlled by π-electron conjugation along the conjugated backbone. The UV/VIS spectra no longer resemble those of DEE dimer **13** or homo-trimer **12**. Furthermore, the first reduction is now greatly facilitated, not only

with respect to **12** and **13**, but also in comparison with the pure spacer chromophores. For example, the first reduction step of hybrid trimer **14** is anodically shifted by 490 mV with respect to the reduction of benzothiadiazole **43** and by 410 mV with respect to the DEE homo-trimer **12**. We propose that, in these systems, the two DEE moieties act as strongly electron-withdrawing substituents of the spacer chromophore, shifting the potential mainly by inductive effects rather than by delocalization along the oligomeric backbone. Similar electron-withdrawing-substituent effects had previously been postulated to explain the anodic shift by 350 mV measured upon substitution of the two opposite *meso*-positions in a porphyrin derivative by two DEE residues [29]. In conclusion, this study demonstrates two important applications for DEEs: as substituents they dramatically enhance the fluorescence efficiency of larger π-chromophores and greatly facilitate their electron uptake.

Experimental Part

General. Reagents and solvents were purchased reagent grade and used without further purification. Compounds **25** [35], **26** [3], **32** [16], **33** [17][18], and **34** [19][20] were synthesized according to literature procedures; **47** was prepared in analogy to the procedure for **31**, starting from benzene-1,2-diamine and 1,10-phenanthroline-5,6-dione. CH_2Cl_2 was dried over CaH_2, and PhMe and THF over Na. Evaporations and concentrations *in vacuo* were carried out at H_2O-aspirator pressure. M.p.: *Büchi Melting Point B-540*, uncorrected. IR Spectra [cm^{-1}]: *Perkin-Elmer 1600-FTIR*, measured in $CHCl_3$, CCl_4, or in KBr pellets. UV/VIS Spectra (λ_{max} [nm] (ε [M^{-1} cm^{-1}])): *Varian Cary-5 UV/VIS/NIR* and *Varian Cary-500 UV/VIS/NIR* spectrophotometer at r.t. Fluorescence spectra (λ_{em} [nm]): *SPEX-1680 Fluorolog 0.22m Double Spectrophotometer* at r.t. Anthracene in hexane was used as reference compound in quantum-yield determinations [24]. ^{1}H- and ^{13}C-NMR Spectra [ppm]: *Bruker AMX-500*, *Varian Gemini-200* and *-300* at r.t. in $CDCl_3$; solvent peaks (7.24 ppm for ^{1}H and 77.0 ppm for ^{13}C) as internal reference. MS (*m/z* (%)); EI: *VG Tribrid* mass spectrometer at 70 eV ionization energy; MALDI-TOF-MS: *Bruker Reflex-MALDI-TOF* (337-nm N_2-laser system, 2,5-dihydroxybenzoic acid (DHB) as matrix); FT-ICR-MALDI-MS: *Ion Spec Ultima FT-ICR-MS* (337-nm N_2-laser system, DHB and {(2*E*)-3-[(4-*tert*-butyl)phenyl]-2-methylprop-2-enylidene}malononitrile (DCTB) as matrix).

Electrochemistry. CH_2Cl_2 was purchased spectral grade from *Merck*, dried over molecular sieves (4 Å), and stored under Ar. Bu_4NPF_6 was purchased electrochemical grade from *Fluka* and used as received. The electrochemical experiments were carried out at 20° in CH_2Cl_2 containing 0.1M Bu_4NPF_6 in a classical three-electrode cell. The working electrode was a glassy-C disk electrode (3 mm in diameter) and was used either in a motionless mode for CV (0.1 to 10 V s^{-1}) or as a rotating-disk electrode for RDV. The auxiliary electrode was a Pt wire, and the pseudo-reference electrode used was also a Pt wire. All potentials are referenced to the ferricinium/ferrocene (Fc^+/Fc) couple used as an internal standard. The accessible range of potentials on the glassy-C electrode was +1.4 to −2.4 V *vs.* Fc^+/Fc in CH_2Cl_2. The electrochemical cell was connected to a computerized multipurpose electrochemical device *AUTOLAB* (*Eco Chemie BV*, Utrecht, The Netherlands) controlled by the *GPSE* software running on a personal computer.

4,7-Dibromobenzo[1,2,5]thiadiazole (**27**) [36]. A mixture of 1,2,5-benzothiadiazole (20.0 g, 147 mmol) in aq. HBr (48%, 60 ml) was heated to reflux with stirring, while Br_2 (22.6 ml, 440 mmol) was added slowly within 1 h. Towards the end of the addition, the mixture became a suspension. To facilitate stirring, aq. HBr (48%, 40 ml) was added, and the mixture was heated to reflux for 2 h after completion of the Br_2 addition. The mixture was filtered while hot, cooled, filtered again, and washed well with H_2O. The compound was dried (Na_2SO_4) and recrystallized (MeOH) to give **27** (38.0 g, 88%). White needles. M.p. 188–189°. IR (KBr): 3078*w*, 3033*w*, 1857*w*, 1661*w*, 1595*w*, 1500*w*, 1482*m*, 1315*m*, 1272*w*, 1190*s*, 940*s*, 881*s*, 845*m*, 828*s*, 589*s*, 489*s*. ^{1}H-NMR ($CDCl_3$, 200 MHz): 7.71 (*s*, 2 H). ^{13}C-NMR ($CDCl_3$, 50 MHz): 113.95; 132.42; 153.06. EI-MS: 294.0 (100, M^+), 215.1 (28), 134.1 (17). Anal. calc. for $C_6H_2Br_2N_2S$ (293.97): C 24.51, H 0.69, N 9.53, S 10.91; found: C 24.73, H 0.71, N 9.35, S 10.71.

3,6-Dibromobenzene-1,2-diamine (**36**) [37]. To a suspension of **27** (5.0 g, 17 mmol) in EtOH (170 ml), $NaBH_4$ (11.4 g, 300 mmol) was added portionwise at 0°, and the mixture was stirred for 20 h at r.t. After evaporation *in vacuo*, H_2O (100 ml) was added, and the mixture was extracted with Et_2O. The org. phase was washed with sat. aq. NaCl soln. and dried (Na_2SO_4). Evaporation *in vacuo* gave **36** (3.9 g, 87%). White solid.

M.p. 94–95°. IR (KBr): 3390*m*, 3356*m*, 3312*m*, 3244*m*, 1817*w*, 1650*s*, 1611*m*, 1561*m*, 1450*s*, 1250*m*, 1137*m*, 1071*m*, 867*m*, 762*s*. ^{1}H-NMR ($CDCl_3$, 300 MHz): 3.89 (br. *s*, 4 H); 6.84 (*s*, 2 H). ^{13}C-NMR ($CDCl_3$, 75 MHz): 109.74; 123.33; 133.83. EI-MS: 265.9 (100, M^+), 185.0 (8), 157.9 (5), 105.0 (12), 78 (8), 52 (6).

5,8-Dibromoquinoxaline (**28**). An aq. soln. of glyoxal (40%, 0.825 g, 5.6 mmol) was added dropwise to **36** (1.5 g, 5.6 mmol) in EtOH (38 ml). The mixture was heated to reflux for 3 h, cooled, and the pale-yellow precipitate was separated by filtration. Recrystallization (Me_2CO) gave **28** (0.65 g, 40%). Pale-yellow needles. M.p. 227°. IR (KBr): 3423*w* (br.), 3070*w*, 3038*w*, 2359*w*, 2321*w*, 1869*w*, 1647*w*, 1583*w*, 1465*m*, 1431*m*, 1373*m*, 1170*m*, 1025*m*, 973*s*, 880*m*, 822*m*, 578*m*, 484*m* 419*w*. ^{1}H-NMR ($CDCl_3$, 300 MHz): 8.01 (*s*, 2 H); 9.02 (*s*, 2 H). ^{13}C-NMR ($CDCl_3$, 75 MHz): 123.98; 133.73; 141.57; 146.04. EI-MS: 288.0 (100, M^+), 261.0 (14), 233.9 (25), 209.0 (7), 181.0 (2), 153.0 (8), 100.0 (6), 74.0 (7). Anal. calc. for $C_8H_4Br_2N_2$ (287.94): C 33.37, H 1.40, N 9.73; found: C 33.64, H 1.25, N 9.53.

5,8-Dibromo-2,3-diphenylquinoxaline (**29**). A soln. of **36** (1.0 g, 3.8 mmol) and benzil (0.80 g, 3.8 mmol) in EtOH (40 ml) was heated to reflux for 1 h, then cooled to 0°. The formed precipitate was isolated by filtration and washed with EtOH to afford **29** (1.16 g, 70%). White solid. M.p. 221–222°. IR (KBr): 3095*w*, 3056*w*, 1869*w*, 1650*w*, 1583*w*, 1539*w*, 1494*w*, 1450*m*, 1417*w*, 1381*m*, 1333*m*, 1300*m*, 1286*w*, 1262*w*, 1238*w*, 1214*m*, 1172*s*, 1107*w*, 1077*w*, 1061*m*, 1024*m*, 1000*m*, 983*s*, 929*w*, 894*m*, 855*w*, 828*m*, 772*s*, 738*w*, 714*w*, 694*s*, 656*m*, 631*w*, 613*w*, 595*w*, 578*m*, 533*m*. ^{1}H-NMR ($CDCl_3$, 200 MHz): 7.3–7.5 (*m*, 6 H); 7.6–7.7 (*m*, 4 H); 7.92 (*s*, 2 H). ^{13}C-NMR ($CDCl_3$, 50 MHz): 123.73; 128.36; 129.57; 130.24; 133.10; 137.95; 139.35; 154.14. EI-MS: 440.0 (100, M^+), 361.1 (4), 337.0 (19), 279.2 (7), 258.1 (23), 177.1 (22). Anal. calc. for $C_{20}H_{12}Br_2N_2$ (440.14): C 54.58, H 2.75, N 6.36; found: C 54.59, H 2.89, N 6.53.

*10,13-Dibromodibenzo[*a,c*]phenazine* (**30**). A soln. of **36** (1.03 g, 3.9 mmol) and phenanthrene-9,10-dione (0.81 g, 3.9 mmol) in EtOH/AcOH 20:1 (42 ml) was heated to reflux for 2 h, then cooled to 0°. The precipitate formed was isolated by filtration and washed with EtOH to afford **30** (1.37 g, 80%). Yellow solid. M.p. 316–317°. IR (KBr): 3066*m*, 1860*w*, 1654*w*, 1604*m*, 1599*m*, 1580*m*, 1492*m*, 1453*s*, 1438*m*, 1378*m*, 1348*s*, 1332*s*, 1321*m*, 1290*m*, 1222*m*, 1178*s*, 1167*m*, 1126*m*, 1074*m*, 1038*m*, 986*s*, 969*w*, 900*s*, 866*m*, 840*m*, 823*m*, 761*s*, 724*s*, 704*m*, 666*m*, 545*s*, 440*m*. ^{1}H-NMR ($CDCl_3$, 300 MHz): 7.79 (*dt*, $J = 7.8, 1.5, 2$ H); 7.85 (*dt*, $J = 7.8, 1.5, 2$ H); 8.04 (*s*, 2 H); 8.57 (*dd*, $J = 7.8, 1.5, 2$ H); 9.48 (*dd*, $J = 7.8, 1.5, 2$ H). ^{13}C-NMR ($CDCl_3$, 75 MHz): 123.10; 124.23; 127.29; 128.39; 129.57; 131.30; 132.68; 132.92; 143.53; one peak missing. EI-MS: 438.0 (100, M^+), 359.0 (8), 277.1 (15), 251.1 (4). Anal. calc. for $C_{20}H_{10}Br_2N_2$ (438.12): C 54.83, H 2.30, N 6.39; found: C 54.98, H 2.46, N 6.64.

1,10-Phenanthroline-5,6-dione (**37**). To a stirred soln. of 1,10-phenanthroline monohydrate (5.0 g, 27.8 mmol) in $CHCl_3$ (35 ml) and commercial bleach (125 ml, pH 8.5, adjusted with conc. HCl), Bu_4NHSO_4 (4.2 g, 12.4 mmol) was added. The soln. was cooled with a water-bath and vigorously stirred for 6 h. The two phases were separated, and the aq. phase was extracted with $CHCl_3$ (2×100 ml). The combined org. phases were washed with H_2O (100 ml), dried ($MgSO_4$), and evaporated *in vacuo*. $H_2SO_4/HNO_3/H_2O$ (25 ml, 6:3:1) was added to the yellow solid residue, and the mixture was heated to 120° until the red-brown vapor disappeared. The yellow soln. was carefully neutralized with conc. NaOH and sat. aq. K_2CO_3 solns. while cooling in an ice-bath and then extracted with $CHCl_3$ (3×100 ml). The combined org. phases were washed with H_2O (100 ml), dried ($MgSO_4$), and evaporated *in vacuo*. The residue was recrystallized from MeOH to afford **37** (1.3 g, 22%). Yellow solid. M.p. 258–259°. IR (KBr): 3060*m*, 1702*m*, 1685*s*, 1578*s*, 1560*s*, 1522*m*, 1458*s*, 1414*s*, 1356*m*, 1317*m*, 1293*s*, 1274*m*, 1204*m*, 1115*m*, 1083*m*, 1056*m*, 1011*m*, 925*m*, 806*m*, 738*s*, 672*w*, 611*w*, 533*w*. ^{1}H-NMR ($CDCl_3$, 300 MHz): 7.58 (*dd*, $J = 7.8, 4.7, 2$ H); 8.50 (*dd*, $J = 7.8, 1.9, 2$ H); 9.12 (*dd*, $J = 4.7, 1.9, 2$ H). ^{13}C-NMR ($CDCl_3$, 75 MHz): 125.68; 128.19; 137.41; 153.07; 156.55; 178.87. EI-MS: 210.0 (6, M^+), 182.1 (100). Anal. calc. for $C_{12}H_6N_2O_2 \cdot 0.2\ H_2O$ (213.79): C 67.42, H 3.02, N 13.10; found: C 67.29, H 3.18, N 13.42.

*10,13-Dibromodipyrido[3,2-*a*:2,3-*c*]phenazine* (**31**). Compound **36** (0.53 g, 2.0 mmol) was added in one portion to a suspension of **37** (0.42 g, 2.0 mmol) in EtOH (25 ml), and the mixture was stirred at reflux for 3 h. The soln. turned black initially, and afterwards a pale-yellow precipitate was obtained. After cooling the mixture, filtration afforded a solid, which was washed with Me_2CO (20 ml) and Et_2O (40 ml) to give **31** (0.364 g, 91%). Yellow solid. M.p. >400°. IR (KBr): 3067*m*, 3012*m*, 2350*w*, 1961*w*, 1923*w*, 1895*w*, 1708*w*, 1580*m*, 1560*m*, 1474*s*, 1459*m*, 1439*s*, 1411*s*, 1348*s*, 1311*s*, 1224*s*, 1175*m*, 1120*s*, 1065*s*, 1032*s*, 988*s*, 984*s*, 850*m*, 804*s*, 739*s*, 707*m*, 658*m*, 592*m*, 540*m*, 493*w*, 438*m*. ^{1}H-NMR ($CDCl_3$, 300 MHz): 7.86 (*dd*, $J = 8.1, 4.4, 2$ H); 8.12 (*s*, 2 H); 9.33 (*dd*, $J = 4.4, 1.9, 2$ H); 9.74 (*dd*, $J = 8.1, 1.9, 2$ H). EI-MS: 440.0 (60, M^+), 413.0 (3), 360.1 (8), 332.1 (2), 279.2 (6), 18 (100). Anal. calc. for $C_{18}H_8Br_2N_4$ (440.10): C 49.13, H 1.83, N 12.73; found: C 49.19, H 1.94, N 12.89.

General Procedure for Sonogashira *Cross-Coupling Reactions.* To a degassed soln. of **25** (0.15 g, 3.13 mmol) and **27**, **28**, **29**, or **30** (37 mg, 50 mg, 57 mg, or 57 mg, respectively, 1.30 mmol) in dry CH_2Cl_2 (5 ml) and freshly distilled Et_3N (5 ml) under Ar, $[PdCl_2(PPh_3)_2]$ (5 mol-%) and CuI (6 mol-%) were added at once at r.t. (**27** or **28**) or at reflux (**29** or **30**). The soln. was stirred at r.t. (**27** or **28**) or at reflux (**29** or **30**) for 18 h. The mixture was

passed through a plug of SiO_2-*60* (10×2 cm, CH_2Cl_2). Evaporation *in vacuo* and chromatography (SiO_2-*60*; hexane/CH_2Cl_2 1:1 → 1:2 → pure CH_2Cl_2) afforded **14** (0.10 g, 70%), **15** (0.09 g, 48%), **16** (0.07 g, 43%), and **17** (0.09 g, 56%).

*4,7-Bis((*E*)-3,4-bis[[(*tert*-butyl)dimethylsilyloxy]methyl]-6-(triethylsilyl)hex-3-ene-1,5-diynyl)-2,1,3-benzothiadiazole* (**14**). Orange-red solid. M.p. 120–121°. UV/VIS (CH_2Cl_2): 251 (24700), 319 (sh, 39700), 330 (42900), 438 (35900). IR (KBr): 3444*s* (br.), 2956*s*, 2939*m*, 2881*m*, 2189*w*, 2133*w*, 1656*w*, 1633*w*, 1562*w*, 1491*w*, 1479*w*, 1461*m*, 1414*w*, 1385*w*, 1361*w*, 1250*m*, 1178*w*, 1130*m*, 1100*m*, 1041*w*, 1018*w*, 1006*m*, 970*w*, 947*w*, 923*w*, 833*s*, 817*m*, 772*m*, 722*m*. ^{1}H-NMR ($CDCl_3$, 500 MHz): 0.14 (*s*, 24 H); 0.66 (*q*, $J = 7.9$, 12 H); 0.940 (*s*, 18 H); 0.944 (*s*, 18 H); 1.03 (*t*, $J = 7.9$, 18 H); 4.63 (*s*, 4 H); 4.74 (*s*, 4 H); 7.62 (*s*, 2 H). ^{13}C-NMR ($CDCl_3$, 125 MHz): −5.13; −5.10; 4.35; 7.50; 18.43; 18.48; 25.93; 25.99; 63.85; 64.20; 95.11; 97.09; 102.91; 105.95; 117.28; 130.13; 131.65; 154.41. FT-ICR-MALDI-MS (DHB, 2-layer): 1111.591 (100, $[M + Na]^+$, $C_{58}H_{100}N_2NaO_4SSi_6^+$; calc. 1111.592), 981 (5), 849 (4). Anal. calc. for $C_{58}H_{100}N_2O_4SSi_6$ (1090.02): C 63.91, H 9.25, N 2.57, S 2.94; found: C 63.85, H 9.07, N 2.43, S 2.85.

*5,8-Bis((*E*)-3,4-bis[[(*tert*-butyl)dimethylsilyloxy]methyl]-6-(triethylsilyl)hex-3-ene-1,5-diynyl)quinoxaline* (**15**). Yellow solid. M.p. 106–107°. UV/VIS (CH_2Cl_2): 264 (33100), 322 (30500), 409 (31300), 436 (sh, 22300). IR (CCl_4): 2955*s*, 2932*m*, 2880*m*, 2858*m*, 2197*w*, 2133*w*, 1562*w*, 1487*w*, 1472*m*, 1462*m*, 1413*w*, 1391*w*, 1361*w*, 1347*w*, 1323*w*, 1282*w*, 1254*m*, 1172*w*, 1100*m*, 1050*m*, 1006*m*, 975*w*, 938*w*, 839*s*, 816*w*, 809*w*. ^{1}H-NMR ($CDCl_3$, 300 MHz): 0.14 (*s*, 12 H); 0.15 (*s*, 12 H); 0.66 (*q*, $J = 7.8$, 12 H); 0.94 (*s*, 18 H); 0.95 (*s*, 18 H); 1.04 (*t*, $J = 7.8$, 18 H); 4.65 (*s*, 4 H); 4.77 (*s*, 4 H); 7.83 (*s*, 2 H); 8.89 (*s*, 2 H). ^{13}C-NMR ($CDCl_3$, 75 MHz): −5.30 (2×); 4.22; 7.36; 18.31 (2×); 25.82; 25.86; 63.94; 64.18; 95.13; 97.95; 103.09; 105.52; 124.26; 130.54; 131.30; 132.99; 143.35; 145.50. FT-ICR-MALDI-MS (DHB, 2-layer): 1105.635 (100, $[M + Na]^+$, $C_{60}H_{102}N_2NaO_4Si_6^+$; calc. 1105.635). Anal. calc. for $C_{60}H_{102}N_2O_4Si_6$ (1083.99): C 66.48, H 9.48, N 2.58; found: C 66.72, H 9.64, N 2.75.

*5,8-Bis((*E*)-3,4-bis[[(*tert*-butyl)dimethylsilyloxy]methyl]-6-(triethylsilyl)hex-3-ene-1,5-diynyl)-2,3-diphenylquinoxaline* (**16**). Yellow solid. M.p. 69–70°. UV/VIS (CH_2Cl_2): 269 (35400), 315 (42000), 321 (41900), 396 (sh, 28500), 416 (29900), 435 (sh, 24100). IR (CCl_4): 2957*m*, 2930*m*, 2877*m*, 2856*m*, 2198*w*, 2132*w*, 1557*w*, 1497*w*, 1472*w*, 1462*w*, 1445*w*, 1414*w*, 1378*w*, 1361*w*, 1343*w*, 1281*w*, 1254*m*, 1172*w*, 1131*w*, 1101*m*, 1054*w*, 1018*w*, 1006*w*, 975*w*, 939*w*, 909*w*, 839*s*, 812*m*, 808*s*. ^{1}H-NMR ($CDCl_3$, 300 MHz): −0.09 (*s*, 12 H); 0.13 (*s*, 12 H); 0.67 (*q*, $J = 8.0$, 12 H); 0.81 (*s*, 18 H); 0.94 (*s*, 18 H); 1.04 (*t*, $J = 8.0$, 18 H); 4.65 (*s*, 4 H); 4.78 (*s*, 4 H); 7.3–7.4 (*m*, 6 H); 7.58–7.64 (*m*, 4 H); 7.82 (*s*, 2 H). ^{13}C-NMR ($CDCl_3$, 75 MHz): −5.38; −5.27; 4.22; 7.26; 18.04; 18.30; 25.72; 25.80; 64.12; 64.33; 95.00; 98.39; 103.39; 105.21; 123.86; 128.20; 129.18; 130.36; 130.97; 131.04; 132.80; 138.94; 141.20; 153.67. FT-ICR-MALDI-MS (DHB, 2-layer): 1258.699 (100, $[M + Na]^+$, $C_{72}H_{110}N_2NaO_4Si_6^+$; calc. 1258.701). Anal. calc. for $C_{72}H_{110}N_2O_4Si_6$ (1236.19): C 69.96, H 8.97, N 2.27; found: C 69.87, H 8.75, N 2.29.

*10,13-Bis((*E*)-3,4-bis[[(*tert*-butyl)dimethylsilyloxy]methyl]-6-(triethylsilyl)hex-3-ene-1,5-diynyl)dibenzo[*a,c*]phenazine* (**17**). Yellow-green solid. M.p. 125°. UV/VIS (CH_2Cl_2): 254 (68900), 304 (sh, 41200), 316 (49000), 328 (sh, 45800), 395 (sh, 19700), 416 (26700), 445 (sh, 21300). IR (KBr): 3456*m* (br.), 2956*s*, 2934*s*, 2886*m*, 2856*m*, 2133*w*, 1497*w*, 1472*m*, 1456*w*, 1394*w*, 1385*w*, 1373*w*, 1355*w*, 1278*w*, 1256*m*, 1172*w*, 1094*s*, 1047*w*, 1006*w*, 970*w*, 935*w*, 911*w*, 839*s*, 817*m*, 778*m*, 763*m*, 722*m*, 711*m*, 686*w*, 550*w*. ^{1}H-NMR ($CDCl_3$, 500 MHz): 0.03 (*s*, 12 H); 0.16 (*s*, 12 H); 0.69 (*q*, $J = 8.1$, 12 H); 0.84 (*s*, 18 H); 0.93 (*s*, 18 H); 1.06 (*t*, $J = 8.1$, 18 H); 4.75 (*s*, 4 H); 4.90 (*s*, 4 H); 7.76 (*dd*, $J = 7.5$, 7.5, 2 H); 7.82 (*ddd*, $J = 7.5$, 7.5, 1.5, 2 H); 7.94 (*s*, 2 H); 8.58 (*d*, $J = 7.5$, 2 H); 9.47 (*dd*, $J = 7.5$, 1.5, 2 H). ^{13}C-NMR ($CDCl_3$, 75 MHz): −5.17; 4.27; 7.41; 18.15; 18.33; 25.79; 25.84; 63.36; 64.44; 94.97; 98.90; 103.35; 105.34; 122.96; 124.11; 127.14; 128.19; 130.18; 130.78; 131.21; 132.53; 133.01; 141.97; 142.85. FT-ICR-MALDI-MS (DHB, 2-layer): 1256.684 (100, $[M + Na]^+$, $C_{72}H_{108}N_2NaO_4Si_6^+$; calc. 1256.686), 1234.7 (10), 1102.6 (35), 969.5 (83). Anal. calc. for $C_{72}H_{108}N_2O_4Si_6$ (1234.17): C 70.07, H 8.82, N 2.27; found: C 70.24, H 8.69, N 2.22.

*10,13-Bis((*E*)-3,4-bis[[(*tert*-butyl)dimethylsilyloxy]methyl]-6-(triethylsilyl)hex-3-ene-1,5-diynyl)dipyrido[3,2-*a:*2,3-*c*]phenazine* (**18**). To a well-degassed soln. of **25** (0.5 g, 1.04 mmol) in freshly distilled Et_3N (17 ml) and dry CH_2Cl_2 (42 ml) containing **31** (0.23 g, 0.52 mmol) as a suspension, $[PdCl_2(PPh_3)_2]$ (0.036 g, 0.05 mmol) and CuI (0.012 g, 0.06 mmol) were added under reflux in one portion. The mixture was stirred under reflux for 18 h to yield a brownish soln. at the end. Flash chromatography (FC) (SiO_2-*60*; CH_2Cl_2), followed by evaporation *in vacuo* and recrystallization (MeCN), afforded **18** (0.45 g, 68%). Orange solid. M.p. 188–189°. UV/VIS ($CHCl_3$): 253 (85900), 325 (73400), 338 (73900), 397 (20500), 462 (25800). IR (KBr): 3433*w* (br.), 2956*s*, 2936*s*, 2882*m*, 2856*m*, 2356*w*, 2345*w*, 2192*w*, 2133*w*, 1589*w*, 1561*w*, 1537*w*, 1507*w*, 1490*w*, 1472*m*, 1461*m*, 1413*w*, 1389*w*, 1377*w*, 1350*m*, 1324*w*, 1280*w*, 1250*m*, 1217*w*, 1170*w*, 1094*s*, 1051*w*, 1010*m*, 974*w*, 938*w*, 909*w*, 833*s*, 814*m*, 778*s*, 739*m*, 725*m*. ^{1}H-NMR ($CDCl_3$, 500 MHz): 0.05 (*s*, 12 H); 0.16 (*s*, 12 H); 0.70 (*q*, $J = 7.9$, 12 H); 0.86 (*s*, 18 H); 0.92 (*s*, 18 H); 1.07 (*t*, $J = 7.9$, 18 H); 4.77 (*s*, 4 H); 4.86 (*s*, 4 H); 7.81 (*dd*, $J = 8.1$, 4.4, 2 H); 8.00 (*s*, 2 H); 9.30 (*dd*, $J = 4.4$, 1.8, 2 H); 9.71 (*dd*, $J = 8.1$, 1.8, 2 H). ^{13}C-NMR ($CDCl_3$, 75 MHz): −5.02; −4.99; 4.39; 7.54; 18.32; 18.43; 25.88; 25.92; 64.37; 64.45; 95.45; 98.27; 103.08; 105.80; 124.17; 124.32; 127.44; 130.92; 130.96;

133.69; 134.40; 141.46; 142.16; 148.84; 152.95. FT-ICR-MALDI-MS (DHB, 2-layer): 1258.660 (80, $[M+Na]^+$, $^{13}CC_{69}H_{106}N_4NaO_4Si_6^+$; calc. 1258.676), 1236.691 (100, MH^+, $^{13}CC_{69}H_{107}N_4O_4Si_6^+$; calc. 1236.694), 1127.6 (24), 1105.6 (34), 995.5 (14), 989.5 (20), 973.5 (37), 959.5 (56). Anal. calc. for $C_{70}H_{106}N_4O_4Si_6 \cdot 0.5$ AcOEt: C 67.55, H 8.66, N 4.38; found: C 67.54, H 8.35, N 4.12.

General Procedure for the Preparation of the Metal Complexes. To a well-degassed soln. of **18** (41 mg, 0.033 mmol) in $MeOH/CH_2Cl_2$ 1:1 (5 ml), $Zn(OTf)_2$ (6 mg, 0.017 mmol), $Ni(ClO_4)_2 \cdot 6\,H_2O$ (6 mg, 0.017 mmol), or $[Cu(CH_3CN)_4PF_6]$ (6 mg, 0.016 mmol), respectively, were added and the red-colored mixture was protected with Al foil against light and stirred overnight under Ar. Evaporation *in vacuo*, recrystallization (MeOH) at $-20°$, and washing the solids with cold MeOH yielded **19** (30 mg, 64%), **20** (32 mg, 71%), and **21** (25 mg, 58%), respectively.

*Bis[10,13-bis((*E*)-3,4-bis[[(*tert*-butyl)dimethylsilyloxy]methyl]-6-(triethylsilyl)hex-3-ene-1,5-diynyl)dipyrido-[3,2-*a*:2,3-*c*]phenazine]zinc(*II*) Trifluoromethanesulfonate* (**19**). Red solid. M.p. $>240°$ (dec.). UV/VIS ($CHCl_3$): 257 (112300), 324 (sh, 109100), 338 (114400), 395 (22700), 471 (29000). IR (CCl_4): 2957*m*, 2936*w*, 2880*w*, 2859*w*, 2196*w*, 2132*w*, 1578*w*, 1540*w*, 1521*w*, 1493*w*, 1471*w*, 1462*w*, 1421*w*, 1389*w*, 1373*w*, 1354*w*, 1255*m*, 1166*w*, 1100*m*, 1056*w*, 1030*m*, 1006*w*, 974*w*, 939*w*, 917*w*, 839*s*, 638*m*. ^{1}H-NMR ($CDCl_3$, 300 MHz): 0.0–0.2 (*m*, 48 H); 0.6–0.75 (*m*, 24 H); 0.75–0.95 (*m*, 72 H); 1.0–1.1 (*m*, 36 H); 4.65–4.85 (*m*, 16 H); 8.09 (*s*, 4 H); 8.23 (*dd*, $J = 8.1, 5.0$, 4 H); 8.88–8.94 (*m*, 4 H); 9.98–10.2 (*m*, 4 H). ^{13}C-NMR ($CDCl_3$, 125 MHz): −4.99; 4.32; 7.52; 18.36; 25.64; 25.87; 64.34; 64.41; 96.33; 97.24; 102.87; 106.21; 124.42; 129.25; 130.66; 131.23; 134.77; 134.93; 139.54; 142.49; 142.57; 142.60. MALDI-TOF-MS (DCTB): 2688.0 (100, $[M+H-OTf]^+$), 2630.8 (10, $[M+H-OTf-t\text{-}Bu]^+$), 2573.8 (14, $[M+H-2\,OTf+Cl]^+$), 2538.6 (13, $[M+H-2\,OTf]^+$).

*Bis[10,13-bis((*E*)-3,4-bis[[(*tert*-butyl)dimethylsilyloxy]methyl]-6-(triethylsilyl)hex-3-ene-1,5-diynyl)dipyrido-[3,2-*a*:2,3-*c*]phenazine]nickel(*II*) Perchlorate* (**20**). Red solid. M.p. $>250°$ (dec.). UV/VIS ($CHCl_3$): 263 (141300), 342 (158500), 393 (sh, 23500), 485 (32400). IR (CCl_{04}): 2972*s*, 2925*s*, 2853*m*, 2362*w*, 2331*w*, 2196*w*, 2134*w*, 1491*w*, 1473*w*, 1463*w*, 1419*w*, 1353*w*, 1276*w*, 1254*w*, 1172*w*, 1098*m*, 1054*w*, 1007*w*, 977*w*, 941*w*, 918*w*, 838*s*. MALDI-TOF-MS (DCTB): 2629.3 (36, $[M-ClO_4]^+$), 2564.8 (100, $[M-2\,ClO_4+Cl]^+$), 2530.0 (74, $[M-2\,ClO_4]^+$).

*Bis[10,13-bis((*E*)-3,4-bis[[(*tert*-butyl)dimethylsilyloxy]methyl]-6-(triethylsilyl)hex-3-ene-1,5-diynyl)dipyrido-[3,2-*a*:2,3-*c*]phenazine]copper(*I*) Hexafluorophosphate* (**21**). Red-brown solid. M.p. $>235°$ (dec.). UV/VIS ($CHCl_3$): 297 (sh, 120800), 335 (161900), 393 (sh, 32200), 469 (42500). IR ($CHCl_3$): 2952*s*, 2925*s*, 2846*m*, 2194*w*, 2123*w*, 1494*w*, 1463*w*, 1388*w*, 1367*w*, 1355*w*, 1260*s*, 1172*w*, 1098*s*, 1047*m*, 1028*m*, 875*w*, 841*s*, 815*m*, 692*w*. MALDI-TOF-MS (DCTB): 2572.9 (18, $[M-PF_6+Cl]^+$), 2537.4 (100, $[M-PF_6]^+$), 2459.0 (50), 2307.6 (21).

*3,6-Bis((*E*)-3,4-bis[[(*tert*-butyl)dimethylsilyloxy]methyl]-6-(trimethylsilyl)hex-3-ene-1,5-diynyl)pyridazine* (**22**). To a well-degassed soln. of **26** (0.10 g, 0.23 mmol), **33** (0.038 g, 0.11 mmol), Ph_3P (0.86 mg, 0.0028 mmol), and $[PdCl_2(PPh_3)_2]$ (0.0089 g, 0.011 mmol) in THF/$(i\text{-}Pr)_2NH$ (10 ml, 3:1), CuI (0.0022 g, 0.011 mmol) was added. The mixture was stirred at 60° for 21 h, then filtered through a plug (SiO_2-*60*; hexane → hexane/CH_2Cl_2 2:1). Purification by prep. TLC (SiO_2-*60*; hexane/AcOEt 10:1) yielded **22** (0.03 g, 27%). Yellow solid. M.p. 81°. UV/VIS ($CHCl_3$): 351 (45200), 373 (29800). IR ($CHCl_3$): 2953*s*, 2924*s*, 2852*s*, 2201*w*, 2134*w*, 1471*m*, 1461*m*, 1395*m*, 1250*s*, 1099*s*, 937*m*. ^{1}H-NMR (CDCl3, 300 MHz): 0.12 (*s*, 24 H); 0.21 (*s*, 18 H); 0.92 (*s*, 36 H); 4.55 (*s*, 4 H); 4.57 (*s*, 4 H); 7.26 (*d*, $J = 7.2$, 1 H); 7.46 (*d*, $J = 7.2$, 1 H). ^{13}C-NMR ($CDCl_3$, 75 MHz): −5.2; −0.3; 18.3; 25.8; 63.9; 64.0; 92.4; 96.9; 101.4; 108.9; 128.6; 129.1; 133.1; 145.7. FT-ICR-MALDI-MS (DHB, 2-layer): 971.525 (100, $[M+Na]^+$, $C_{50}H_{88}N_2NaO_4Si_6^+$; calc. 971.526).

*5,5′-Bis((*E*)-3,4-bis[[(*tert*-butyl)dimethylsilyloxy]methyl]-6-(trimethylsilyl)hex-3-ene-1,5-diynyl)-2,2′-bithiophene* (**23**). To a well-degassed soln. of **26** (0.1 g, 0.23 mmol), **32** (0.046 g, 0.11 mmol), and $[PdCl_2(PPh_3)_2]$ (5 mg, 0.007 mmol) in Et_3N (2 ml) and dry toluene (5 ml), CuI (3 mg, 0.016 mmol) was added. The mixture was stirred at r.t. for 48 h, then filtered through a plug (SiO_2-*60*; hexane/toluene 1:1). FC (SiO_2-*60*, hexane/CH_2Cl_2 3:1) yielded **23** (0.06 g, 52%). Yellow solid. M.p. 72°. UV/VIS ($CHCl_3$): 273 (14900), 289 (13100), 318 (8600), 338 (11400), 380 (21800), 410 (25200), 447 (13300). IR ($CHCl_3$): 3688*s*, 2953*m*, 2904*m*, 2838*m*, 2106*w*, 1601*s*, 1073*m*, 844*s*. ^{1}H-NMR ($CDCl_3$, 300 MHz): 0.12 (*s*, 24 H); 0.21 (*s*, 18 H); 0.94 (*s*, 36 H); 4.47 (*s*, 4 H); 4.54 (*s*, 4 H); 7.04–7.15 (*m*, 4 H). ^{13}C-NMR ($CDCl_3$, 75 MHz): −5.1; −0.2; 18.4; 25.9; 63.9; 64.1; 81.1; 85.6; 102.1; 107.7; 111.2; 122.9; 129.6; 129.9; 130.7; 133.7. FT-ICR-MALDI-MS (DHB, 2-layer): 1034.489 (33, M^+, $C_{54}H_{90}O_4Si_6S_2^+$; calc. 1034.489); 977 (100, $[M-t\text{-}Bu]^+$). Anal. calc. for $C_{54}H_{90}O_4Si_6S_2$ (1035.95): C 62.61, H 8.76; found: C 62.41, H 8.72.

*2,7-Bis((*E*)-3,4-bis[[(*tert*-butyl)dimethylsilyloxy]methyl]-6-(trimethylsilyl)hex-3-ene-1,5-diynyl)-9,9′-dioctyl-9H-fluorene* (**24**). To a well-degassed soln. of **26** (0.102 g, 0.23 mmol), **34** (0.050 g, 0.09 mmol), Ph_3P (1.2 mg, 0.0046 mmol), and $[PdCl_2(PPh_3)_2]$ (19 mg, 0.0028 mmol) in Et_3N (10 ml), CuI (1.0 mg, 0.0055 mmol) was added. The mixture was stirred at 70° for 23 h, then filtered through a plug (SiO_2-*60*; hexane/CH_2Cl_2 1:1). FC

(SiO_2-*60*; hexane/CH_2Cl_2 1:1) yielded **24** (0.10 g, 85%). Yellow solid. M.p. 54°. UV/VIS ($CHCl_3$): 273 (17200), 323 (20000), 375 (60000), 392 (46400). IR ($CHCl_3$): 2930*m*, 2856*s*, 2133*w*, 1465*s*, 1252*m*, 1103*m*, 843*s*. ^{1}H-NMR ($CDCl_3$, 300 MHz): 0.14 (*s*, 24 H); 0.23 (*s*, 18 H); 0.59 (*m*, 4 H); 0.82 (*t*, *J* = 6.9, 6 H); 0.97 (*s*, 36 H); 1.05–1.26 (*m*, 20 H); 1.86–1.98 (*m*, 4 H); 4.58 (*s*, 8 H); 7.41 (*s*, 2 H); 7.42 (*d*, *J* = 8.4, 2 H); 7.63 (*d*, *J* = 8.4, 2 H). ^{13}C-NMR ($CDCl_3$, 75 MHz): −5.1; −0.1; 14.1; 18.5; 22.6; 23.8; 26.0; 29.3; 30.1; 31.8; 40.4; 55.2; 64.2; 87.3; 102.3; 102.7; 107.1; 120.2; 122.3; 126.3; 129.1; 130.7; 131.4; 141.1; 151.4. FT-ICR-MALDI-MS (DHB, 2-layer): 1281.819 (100, $[M+Na]^+$, $C_{75}H_{126}NaO_4Si_6^+$; calc. 1281.817), 1258 (9, M^+). Anal. calc. for $C_{75}H_{126}O_4Si_6$ (1260.35): C 71.48, H 10.08; found: C 71.49, H 10.25.

This work was supported by the *ETH Research Council*. Financial support of the NCCR Nanoscale Science is also gratefully acknowledged. We thank *B. Stump, M. Zanni*, and *I. Rybicki* for synthetic contributions during the advanced organic laboratory course OCP2.

REFERENCES

[1] R. E. Martin, J. A. Wytko, F. Diederich, C. Boudon, J.-P. Gisselbrecht, M. Gross, *Helv. Chim. Acta* **1999**, *82*, 1470.
[2] R. E. Martin, U. Gubler, C. Boudon, V. Gramlich, C. Bosshard, J.-P. Gisselbrecht, P. Günter, M. Gross, F. Diederich, *Chem. – Eur. J.* **1997**, *3*, 1505.
[3] R. E. Martin, U. Gubler, J. Cornil, M. Balakina, C. Boudon, C. Bosshard, J.-P. Gisselbrecht, F. Diederich, P. Günter, M. Gross, J.-L. Brédas, *Chem. – Eur. J.* **2000**, *6*, 3622.
[4] M. J. Edelmann, M. A. Estermann, V. Gramlich, F. Diederich, *Helv. Chim. Acta* **2001**, *84*, 473.
[5] M. J. Edelmann, S. Odermatt, F. Diederich, *Chimia* **2001**, *55*, 132.
[6] P. Siemsen, R. C. Livingston, F. Diederich, *Angew. Chem.* **2000**, *112*, 2740; *Angew. Chem., Int. Ed.* **2000**, *39*, 2632; A. S. Hay, *J. Org. Chem.* **1962**, *27*, 3320.
[7] S. Takahashi, Y. Kuroyama, K. Sonogashira, N. Hagihara, *Synthesis* **1980**, 627; K. Sonogashira, in 'Metal-catalyzed Cross-coupling Reactions', Eds. F. Diederich, P. J. Stang, Wiley-VCH, Weinheim, 1998, pp. 203–230.
[8] H. A. Dieck, F. R. Heck, *J. Organomet. Chem.* **1975**, *93*, 259.
[9] R. Diaz, O. Reyes, A. Francois, A. M. Leiva, B. Loeb, *Tetrahedron Lett.* **2001**, *42*, 6463.
[10] M. Yamada, Y. Tanaka, Y. Yoshimoto, S. Kuroda, I. Shimao, *Bull. Chem. Soc. Jpn.* **1992**, *65*, 1006.
[11] J. E. Dickeson, L. A. Summers, *Aust. J. Chem.* **1970**, *23*, 1023.
[12] R. Lopez, B. Loeb, T. Boussie, T. J. Meyer, *Tetrahedron Lett.* **1996**, *37*, 5437.
[13] C. J. Moody, C. W. Rees, R. Thomas, *Tetrahedron* **1992**, *48*, 3589.
[14] E. Amouyal, A. Homsi, J.-C. Chambron, J.-P. Sauvage, *J. Chem. Soc., Dalton Trans.* **1990**, *19*, 1841.
[15] J. Druey, P. Schmidt, *Helv. Chim. Acta* **1950**, *33*, 1080.
[16] L. L. Miller, Y. Yu, *J. Org. Chem.* **1995**, *60*, 6813.
[17] M. S. Shin, Y. J. Kang, H. A. Chung, J. W. Park, D. H. Kweon, W. S. Lee, Y. J. Yoon, S. K. Kim, *J. Heterocycl. Chem.* **1999**, *36*, 1135.
[18] R. H. Mizzoni, P. E. Spoerri, *J. Am. Chem. Soc.* **1951**, *73*, 1873.
[19] S. Setayesh, A. C. Grimsdale, T. Weil, V. Enkelmann, K. Müllen, F. Meghdadi, E. J. W. List, G. Leising, *J. Am. Chem. Soc.* **2001**, *123*, 946.
[20] S. Setayesh, D. Marsitzky, K. Müllen, *Macromolecules* **2000**, *33*, 2016.
[21] J. E. Huheey, 'Anorganische Chemie. Prinzipien von Struktur und Reaktivität', Walter de Gruyter, Berlin, 1988.
[22] V. V. Osipov, M. N. Usacheva, I. I. Dilung, *Teor. Eksp. Khim.* **1978**, *14*, 703; *Theor. Exp. Chem.* **1978**, *14*, 549.
[23] N. I. Rtishchev, A. N. Dobrodei, A. V. El'tsov, *Zh. Obshch. Khim.* **1999**, *69*, 1731; *Russ. J. Gen. Chem.* **1999**, *69*, 1658.
[24] F. Dörr, H. Gropper, *Ber. Bunsen-Ges. Phys. Chem.* **1963**, *67*, 193.
[25] G. G. Guilbault, in 'Practical Fluorescence', Ed. G. G. Guilbault, Marcel Dekker, New York, 1990, pp. 1–40.
[26] E. Birckner, U. W. Grummt, A. H. Goller, T. Pautzsch, D. A. M. Egbe, M. Al-Higari, E. Klemm, *J. Phys. Chem. A* **2001**, *105*, 10307.
[27] D. A. Skoog, J. J. Leary, 'Molekülfluoreszenz-, Phosphoreszenz- und Chemilumineszenzspektroskopie', Springer-Verlag, Berlin, 1996.

[28] C. E. Halkyard, M. E. Rampey, L. Kloppenburg, S. L. Studer-Martinez, U. H. F. Bunz, *Macromolecules* **1998**, *31*, 8655; T. Miteva, L. Palmer, L. Kloppenburg, D. Neher, U. H. F. Bunz, *Macromolecules* **2000**, *33*, 652.
[29] J. Wytko, V. Berl, M. McLaughlin, R. R. Tykwinski, M. Schreiber, F. Diederich, C. Boudon, J.-P. Gisselbrecht, M. Gross, *Helv. Chim. Acta* **1998**, *81*, 1964.
[30] K. Meerholz, J. Heinze, *Electrochim. Acta* **1996**, *41*, 1839.
[31] A. J. Bard, L. R. Faulkner, in 'Electrochemical Methods: Fundamentals and Applications', John Wiley & Sons, New York, 1980, pp. 488 – 552.
[32] A. Kraft, A. C. Grimsdale, A. B. Holmes, *Angew. Chem.* **1998**, *110*, 416; *Angew. Chem., Int. Ed.* **1998**, *37*, 402.
[33] S.-J. Chung, K.-S. Kim, T.-C. Lin, G. S. He, J. Swiatkiewicz, P. N. Prasad, *J. Phys. Chem. B* **1999**, *103*, 10741 and refs. cit. therein.
[34] M. Albota, D. Beljonne, J.-L. Brédas, J. E. Ehrlich, J.-Y. Fu, A. A. Heikal, S. E. Hess, T. Kogrej, M. D. Levin, S. R. Marder, D. MacCord-Maughon, J. W. Perry, H. Rockel, M. Rumi, G. Subramanian, W. W. Webb, X.-L. Wu, C. Xu, *Science* **1998**, *281*, 1653.
[35] R. R. Tykwinski, M. Schreiber, R. P. Carlon, F. Diederich, V. Gramlich, *Helv. Chim. Acta* **1996**, *79*, 2249.
[36] K. Pilgram, M. Zupan, R. Skiles, *J. Heterocycl. Chem.* **1970**, *7*, 629.
[37] Y. Tsubata, T. Suzuki, T. Miyashi, Y. Yamashita, *J. Org. Chem.* **1992**, *57*, 6749.

Received March 23, 2002